HNUE JOURNAL OF SCIENCE DOI: 10.18173/2354-1059.2021-0034
Natural Sciences 2021, Volume 66, Issue 2, pp. 119-126
This paper is available online at http://stdb.hnue.edu.vn

DEPOSITION OF TRANSPARENT CONDUCTIVITY OF FLUORINE-DOPED SnO_2 THIN FILMS BY SPRAY PYROLYSIS METHOD

Pham Van Vinh[1] and Vu Kim Thai[2]
[1]*Faculty of Physics, Hanoi National University of Education*
[2]*Faculty of Basic Science, the University of Economics - Technology for Industries*

Abstract. SnO_2 and SnO_2:F thin films were successfully deposited on a glass wafer substrate by spray pyrolysis method using $SnCl_2.5H_2O$ and NH_4F as precursors. The effect of deposition temperature and fluorine concentration on the crystal phase formation of SnO_2 was investigated by XRD. The results showed that the films were crystallized in the form of SnO_2 with a tetragonal structure at deposition temperature above 400 ^oC. No XRD peaks related to SnO_2 were found on the films that deposited at a temperature lower than 350 ^oC. The sheet resistance of the SnO_2 films was increased with the increase in the deposition temperature. The crystalline structure of the SnO_2 films did not change in the presence of fluorine impurities while their sheet resistance was significantly decreased. The minimum sheet resistance was 3.7 (Ω/□) corresponding to the samples deposited with the fluorine concentration of 20 wt%. SEM images also showed the crystal shape of SnO_2 in which crystal size decreases with an increase in fluorine concentration. Both SnO_2 and SnO_2:F exhibited good transparent properties in visible light. The bandgap of the SnO_2 films was about 3.90 eV and was slightly expanded when the concentration of fluorine was increased.

Keywords: SnO_2:F, spray pyrolysis, compress sprayer, transparent conductivity.

1. Introduction

SnO_2 is an n-type semiconductor with a wide band gap and high optical transparency. Impurities are often added to increase its conductivity for many applications. Recent studies have shown that when antimony substitutes the cation of tin or fluorine substitutes the anion of oxygen in SnO_2 lattice, the conductivity of the SnO_2 thin film will increase significantly. For this reason, they are often used as doped elements to increase the conductivity of SnO_2 [1-5]. The anion radius of fluorine is quite similar to that of oxygen so it can easily substitute the oxygen vacancies position of the SnO_2 without changing its crystal structure [6, 7]. Therefore, SnO_2:F retains the good transparency of SnO_2 and gets the high conductivity of the doped semiconductor [8]. SnO_2:F is mechanically, chemically, and electrically stable [9], so it can be used as

Received June 10, 2021. Revised June 22, 2021. Accepted June 29, 2021.
Contact Pham Van Vinh, e-mail address: vinhpv@hnue.edu.vn

electrodes for solar cells [10], sensitive layer for gas sensors [11, 12] and transparent electrodes for LCDs [13]. SnO_2 thin films can be deposited by a variety of methods including chemical vapor deposition [14], pulsed laser deposition [15], DC sputtering [5, 16], and spray pyrolysis [17]. Among them, spray pyrolysis has proven to be one of the low-cost and highly effective techniques for thin film deposition. In addition, this technique allows easy doping by adding compounds containing impurities (usual salts) to the sprayed solutions [1, 17, 18]. The optimization of the deposition conditions can be easily done by this method. Normally, an electrostatic and pressure sprayer has been used to spray solutions. Electrostatic sprayer requires the use of high voltage to accelerate spraying solution so it is quite dangerous, especially in high humidity environments like Vietnam. The pressure sprayer has proved safer because it does not need a high voltage source. Therefore, we have used this equipment to deposit the transparent conductivity thin films of SnO_2 and SnO_2:F that are expected to apply for the electrode of solar cells.

2. Content

2.1. Experiments

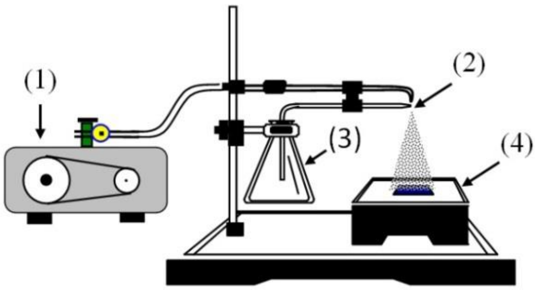

Figure 1. Schematic diagram of experimental apparatus

(1)-Compressor, (2)-Spray nozzle, (3)-Solution tank, (4)-Heater

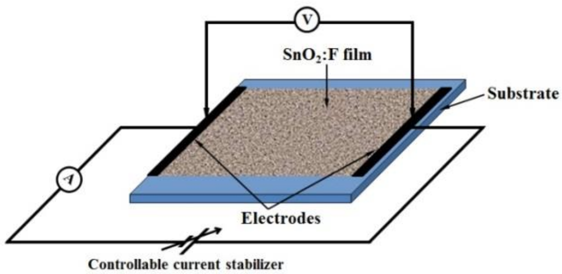

Figure 2. Schematic diagram of sheet resistance measurement

The thin films of SnO_2 and SnO_2:F were deposited by the compress sprayer under the control of the computer. The schematic diagram of the experimental setup published elsewhere [19] is shown in Figure 1. The sprayed solution was prepared by dissolving $SnCl_2.5H_2O$ and NH_4F with the appropriate ratio in an alcohol solution. The hydrochloric acid was added in the solution to prevent the compound from precipitating. The solution was then sprayed on the hot substrate at different temperatures by a compress sprayer. The chemical reactions under heat have created SnO_2 and SnO_2:F thin film. Deposition temperature was carefully studied to find the optimum temperature to deposit the SnO_2 thin films. This temperature was then used to deposit SnO_2:F thin films. The crystal structures were studied by X-ray diffractometer (D8 ADVANCE BRUCKER) with Cu Kα radiation (λ = 0.154056 nm). Surface morphology was observed by SEM (Hitachi S-4800). The optical properties were studied by UV-Vis spectroscopy (Jasco V-670). The sheet resistance was investigated by a homemade system as showing in Figure 2. Two electrodes made of silver conductive paste were attached parallel on the surface of the film. The distance between the two electrodes was equal to the length of the electrode so that the part between the two electrodes was square. The electric current applied between electrodes was provided by a controllable current stabilizer (Keithley). The voltage dropped on the electrodes was measured by a Keithley 2000 multi-meter. The I-V characteristic of the films was investigated to find the sheet resistance (The sheet resistance is the slope of the linear part of the I-V characteristic curve).

2.2. Results and discussions

In order to obtain good transparent conductivity films, it is important to have numerous fluorines substitute for oxygens to generate free electrons. Occupying the position of oxygen in O-Sn-O bonding, fluorine requires appropriate energy to separate oxygen from its bonding. Therefore, this process is difficult to perform. Fluorines can substitute for oxygens easier by occupying the existing oxygen vacancies in the SnO_2 lattice. Thus, it is necessary to find the optimum conditions to deposit the films so that the oxygen vacancies are created the most. Heat is the main factor promoting the crystallization of films. Therefore, heat treatment is believed to be the most effective method of controlling crystal quality as well as defects concentration. Therefore, the effect of deposition temperature on the crystal phase structure and sheet resistance of SnO_2 should be studied as a preparation step for the deposition of SnO_2:F films.

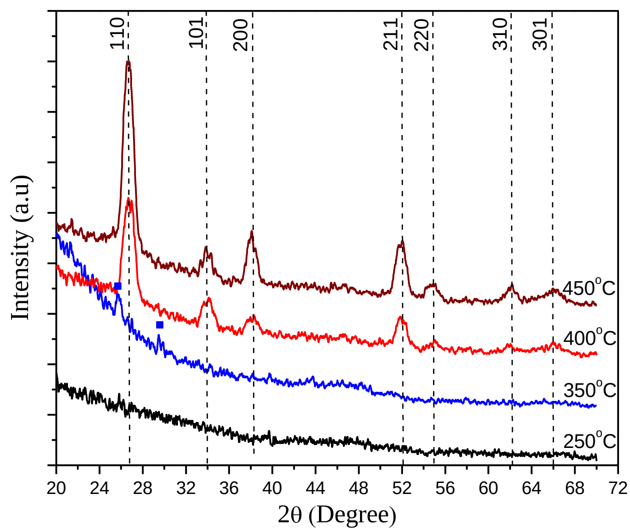

Figure 3. The X-ray diffraction patterns of SnO_2 thin films with different deposition temperature

Figure 3 is the X-ray diffraction patterns of the thin films deposited at different temperatures. There is no XRD peak of the sample deposited at 250^{o}C, indicating that at this temperature, crystalline phases have not been formed. Further increasing the deposition temperature up to 350 ^{o}C, the XRD patterns of the sample have two clear peaks that coincide with the peaks of tin oxide hydroxide crystal (refer to JCPDS No. 25-1303). At this temperature, the sample has begun to crystallize but the temperature is not high enough for the pyrolytic reactions to form SnO_2 crystals. For the deposition temperature over 400 ^{o}C, there are seven XRD peaks of SnO_2 crystals with tetragonal structural (refer to JCPDS No. 41-1445) are found. No diffraction peaks of any other impurities appear. The intensity of diffraction of the peaks is increased with the increase in deposition temperature. These indicate that the films were crystallized better at high temperatures. The pyrolytic reaction is taken place following equations:

$$SnCl_2 + 2C_2H_5OH \longrightarrow Sn(OH)_2 + 2C_2H_5Cl \quad (1)$$

$$Sn(OH)_2 \xrightarrow{t^0} SnO + H_2O \quad (2)$$

$$2SnO + O_2 \xrightarrow{t^0} 2SnO_2 \quad (3)$$

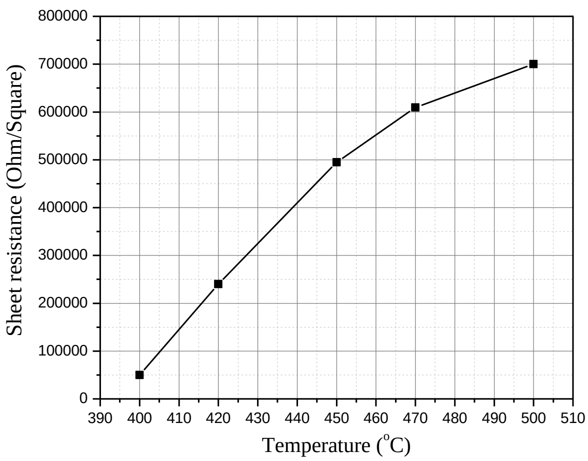

Figure 4. The sheet resistance of the SnO_2 thin films deposited with different temperature

Figure 4 describes the relationship between the sheet resistance of SnO_2 films and deposition temperature. The investigation process was started from the temperature at which SnO_2 crystal begins to form. The sheet resistance increases with the increase in deposition temperature. Perfect SnO_2 has resistance close to the insulator because of its wide bandgap. Somehow, the oxygen vacancies defects generate causes SnO_2 to be an n-type semiconductor. At low deposition temperature, the chemical reactions are not taken place completely and more oxygen vacancies are created, resulting in decreasing the sheet resistance. In contrast, SnO_2 crystal becomes more perfect at high temperatures because of heat so that fewer oxygen vacancies are created. This means that the sheet resistance is high for the films deposited at high temperatures. At 400 °C, the film both crystallized well and has many oxygen vacancies, so this temperature was chosen for further studies.

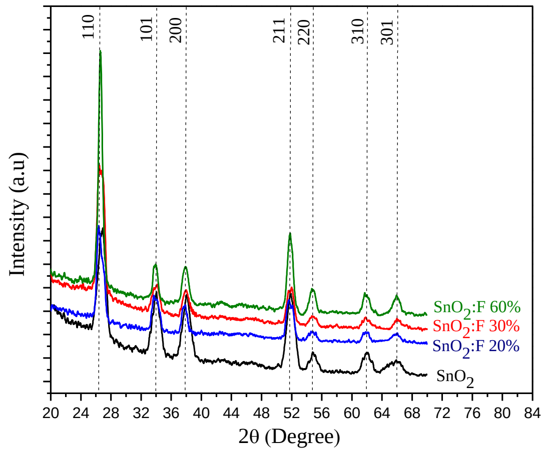

Figure 5. The X-ray diffraction patterns of SnO_2:F thin films deposited at 400 °C with different fluorine concentrations of the precursor solution

Figure 5 shows the X-ray diffraction patterns of SnO_2:F deposited with different fluorine concentrations of the precursor solution. The diffraction patterns show that there are no changes in structure compared to that of SnO_2 samples. Thus, fluorine mainly substitutes for the oxygen in the lattice without causing chemical reactions to form a new structure.

The SEM micrographs of SnO_2:F films deposited with different fluorine concentrations of the precursor solution are shown in Fig. 6. The crystallites have the shape of SnO_2 crystal and are densely packed in which size decreases with an increase in fluorine concentrations. The films deposited at 20 wt% and 30 wt% exhibits fine surfaces with uniform crystals. At higher impurity concentrations, the crystal surface is broken.

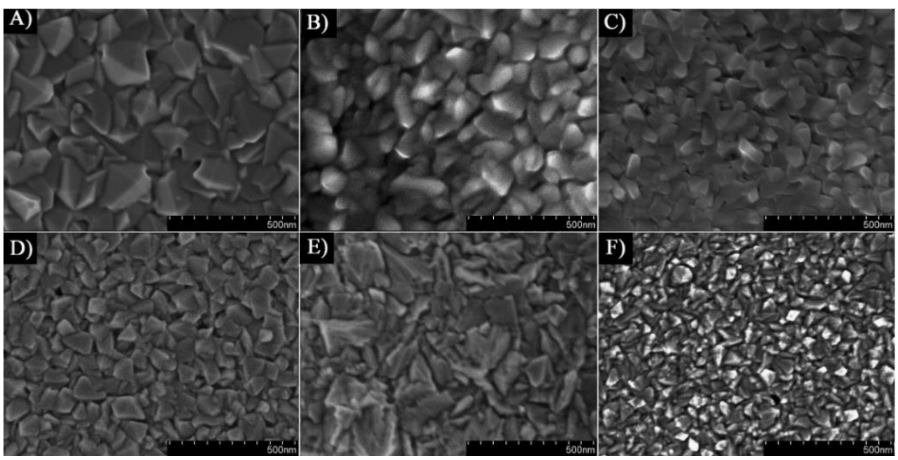

Figure 6. The SEM images of SnO_2:F thin films deposited with different fluorine concentrations of the precursor solution: A)0 wt%; B) 10 wt%; C) 20 wt%; D) 30 wt%; E) 45 wt%; F) 60 wt%

Figure 7 shows the effect of fluorine concentration on the sheet resistance of the SnO_2:F thin films. The results showed that the fluorine concentration significantly affects the sheet resistance. The sheet resistance decreases with the increase in fluorine concentration up to 20 wt%. At this concentration, the sheet resistance was 3.7 (Ω/□). Further increasing fluorine concentration, the sheet resistance increases. The sheet resistance is decided by the density of dopant in the SnO_2 lattice. Increasing fluorine concentration up to 20 wt%, most of the fluorine has been substituted for oxygen in the SnO_2 lattice, providing more free electrons to decrease the sheet resistance. However, if more fluorine is added, the part of the fluorines will act as interstitial defects. This type of defect does not provide free electrons and prevents the charge carrier from moving resulting in increasing sheet resistance.

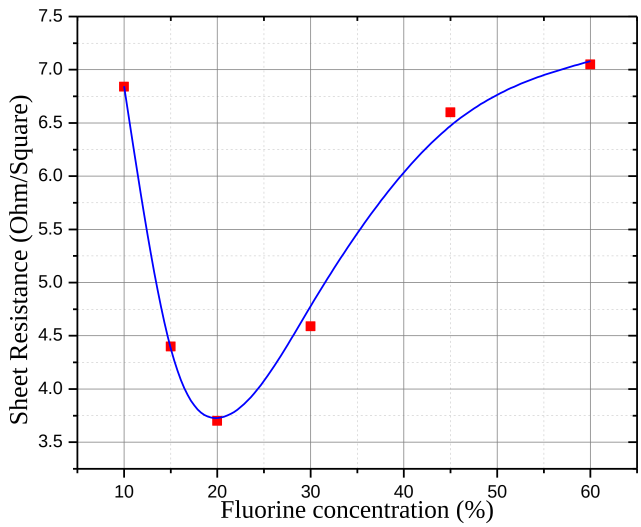

Figure 7. The sheet resistance of the SnO_2:F thin films deposited with different fluorine concentrations of the precursor solution

The optical transmittance and direct allowed transitions of SnO_2:F thin films deposited with different fluorine concentrations are shown in Figures 8A and 8B, respectively. From the transmittance spectra, it is understood that both SnO_2 and SnO_2:F films are good transparences in visible and near-infrared regions. There are some ‘peaks’ appearing on the spectra that are the result of the interference phenomenon. The absolute transmittance value can not be calculated because of the interference peaks. The transmittance is approximately estimated to be 90%.

To study the optical bandgap of the films, the transmittance spectra (Figure 8A) were converted to direct allowed transitions (Figure 8B) under the assistance of the software supported by UV-Vis spectroscopy (Jasco V-670). The optical bandgap was estimated from the extrapolation of the linear portion of the curve to its minimum absorption in the same way as described by Ziad Y. Banyamin *et al.* [20]. The results showed that the bandgap values were about 3.90 eV and increase slightly with the increase in doping concentration. These results agree well with the results that have been reported [15, 21]. With wide bandgap and high doping concentration, the SnO_2:F thin films deposited by the spray pyrolysis method exhibited good transparent conductive properties.

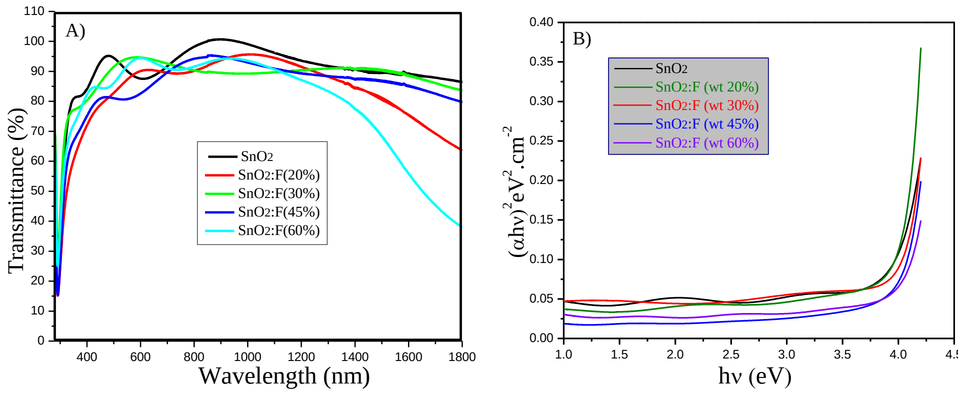

Figure 8. The optical properties of SnO_2:F deposited with different fluorine concentrations of the precursor solution: A) Transmittance spectra, B) Direct allowed transitions

3. Conclusions

Fluorine was doped successfully into the SnO_2 lattice at 400 ^oC by substituting fluorine for oxygen without changing its crystal structure. The crystalline size decreased with the increase in fluorine concentration. The films deposited with the fluorine concentration of 20 wt% and 30 wt% showed fine crystals. The sheet resistance of the films decreased strongly with the presence of fluorine impurity and their value was dependent on fluorine concentration. The minimum value was 3.7 (Ω/□) corresponding to the samples deposited with the fluorine concentration of 20 wt%. Both SnO_2 and SnO_2:F exhibited good transparent properties in the visible region with transmittance up to 90%. The optical bandgap of SnO_2 was about 3.90 eV and went up slightly with the increase in fluorine concentration.

REFERENCES

[1] Supriyono, HediSurahman, Yuni Krisyuningsih, Krisnandi, Jarnuzi, Gunlazuardi, 2015. Preparation and Characterization of Transparent Conductive SnO_2-F Thin Film Deposited by Spray Pyrolysis: Relationship between Loading Level and Some Physical Properties. *Procedia Environmental Sciences*, Vol. 28, pp. 242-251.

[2] Bao-jiaLi, Guang-yu, Yang, Li-jingHuang, WeiZu, Nai-feiRen, 2020. Performance optimization of SnO_2:F thin films under quasi-vacuum laser annealing with covering a transparent PET sheet: A study using processing map. *Applied Surface Science*, Vol. 509, pp.145334.

[3] L.K.Wang, J.J.Chen, J.Y.YuH.L.Zhao, J.K.Yang, 2019. Highly textured spray-deposited SnO_2:F films with high haze for solar cells. *Vacuum*, Vol.169, pp. 108879.

[4] Argelia PérezPacheco, Dwight R.Acosta, CarlosMagaña, 2017. Effect of the amount of the starting solution on physical properties of SnO_2:F thin films. *Surfaces and Interfaces*, Vol. 6, pp. 85-90.

[5] C.Guillén, J.Herrero, 2019. Intrinsic and extrinsic doping contributions in SnO_2 and SnO_2:Sb thin films prepared by reactive sputtering. *Journal of Alloys and Compounds*, Vol. 791, pp. 68-74.

[6] Consonni, V.; Rey, G.; Roussel, H.; Bellet, D. 2012. Thickness Effects on the Texture Development of Fluorine-Doped SnO_2 Thin Films: The Role of Surface and Strain Energy. *J. Appl. Phys.*, Vol. 111, pp. 33523.

[7] Ferrer, F. J.; Gil-Rostra, J.; Terriza, A.; Rey, G.; Jiménez, C.; García-López, J.; Yubero, F., 2012. Quantification of Low Levels of Fluorine Content in Thin Films. Nucl. Instrum. *Methods Phys. Res. Sect. B Beam Interact. Mater. At*., Vol. 274, pp. 65-69.

[8] Subba Ramaiah, K.; Sundara Raja, V., 2006. Structural and electrical properties of fluorine doped tin oxide films prepared by spray-pyrolysis technique. *Appl. Surf. Sci.*, Vol. 253, pp. 1451-1458.

[9] Tesfamichael, T.; Will, G.; Colella, M.; Bell.J., 2003. Optical and electrical properties of nitrogen ion implanted fluorine doped tin oxide films. *Nucl. Instrum. Methods Phys. Res. B Beam Interact. Mater. Atoms*, Vol. 201, pp. 581-588.

[10] Gerhardinger, P.F.; McCurdy, R.J., 1996. Float line deposited transparent conductors-Implications for the PV industry. *MRS Proc.*, Vol. 426, pp. 399-410.

[11] Sankara Subramanian, N.; Santhi, B.; Sundareswaran, S.; Venkatakrishnan, K.S., 2006. Studies on spray deposited SnO_2, Pd:SnO_2 and F:SnO_2 thin films for gas sensor applications. *Synth. React. Inorg. Metal-Org. Nano-Metal Chem*., Vol. 36, pp. 131-135.

[12] Sutichai Chaisitsak, 2011. Nanocrystalline SnO_2:F Thin Films for Liquid Petroleum Gas Sensors, *Sensors*, Vol. 11, pp. 7127-7140.

[13] Yadav, A.A.; Masumdar, E.U.; Moholkar, A.V.; Neumann-Spallart, M.; Rajpure, K.Y.; Bhosale, C.H., 2009. Electrical, structural and optical properties of SnO_2:F thin films: Effect of the substrate temperature. *J. Alloy. Compd*. Vol. 488, pp. 350-355.

[14] Te-HuaFang, Win-JinChang, 2005. Nanomechanical characteristics of SnO_2:F thin films deposited by chemical vapor deposition. *Applied Surface Science*, Vol. 252, pp. 1863-1869.

[15] H.Kim, R.C.Y.AuyeungA.Piqué, 2008. Transparent conducting F-doped SnO_2 thin films grown by pulsed laser deposition. *Thin Solid Films*, Vol. 516, pp. 5052-5056.

[16] T.Jäger,B.Bissig, M.Döbeli, A.N.Tiwari, Y.E.Romanyuk, 2014. Thin films of SnO_2:F by reactive magnetron sputtering with rapid thermal post-annealing. *Thin Solid Films*, Vol. 553, pp. 21-25.

[17] Zahra Mahmoudiamirabad and Hosein Eshghi, 2021. Achievements of high figure of merit and infra-red reflectivity in SnO_2:F thin films using spray pyrolysis technique. *Superlattices and Microstructures*, Vol. 152, pp. 106855.

[18] DengkuiMiao, Qingnan Zhao Shuo Wu, Zhendong Wang, Xingliang Zhang, Xiujian Zhao, 2010. Effect of substrate temperature on the crystal growth orientation of SnO_2:F thin films spray deposited on glass substrates. *Journal of Non-Crystalline Solids*, Vol. 356, pp. 2557-2561.

[19] Pham Van Vinh and Vu Kim Thai, 2021. Deposition and study of alcohol vapor sensitivity of $SnO_2/ZnSnO_3$ thin films. *Scientific Journal*, Vol. 46, pp. 75-84.

[20] Ziad Y. Banyamin, Peter J. Kelly, Glen West and Jeffery Boardman, 2014. Electrical and Optical Properties of Fluorine Doped Tin Oxide Thin Films Prepared by Magnetron Sputtering. *Coatings*, Vol. 4, pp.732-746.

[21] Elangovan, E.; Ramamurthi, K., 2005. Studies on micro-structural and electrical properties of spray-deposited fluorine-doped tin oxide thin films from low-cost precursor. *Thin Solid Films*, Vol. 476, pp. 231-236.